THE ASTROPHYSICAL JOURNAL, 541:126–133, 2000 September 20

STRONG BALMER LINES IN OLD STELLAR POPULATIONS: NO NEED FOR YOUNG AGES IN ELLIPTICALS?

CLAUDIA MARASTON AND DANIEL THOMAS
Universitäts-Sternwarte München, Scheinerstr. 1, D-81679 München, Germany; maraston@usm.uni-muenchen.de, daniel@usm.uni-muenchen.de
Received 1999 November 15; accepted 2000 May 1

ABSTRACT

Comparing models of Simple Stellar Populations (SSPs) with observed line strengths generally provides a tool for breaking the age-metallicity degeneracy in elliptical galaxies. Because of the wide range of Balmer line strengths observed, ellipticals have been interpreted as exhibiting an appreciable scatter in age. In this paper, we analyze Composite Stellar Population models with a simple mix of an old metal-rich and an old metal-poor component. We show that these models simultaneously produce strong Balmer lines and strong metallic lines without invoking a young population. The key to this result is that our models are based on SSPs that better match the steep increase of Hβ in metal-poor globular clusters than models in the literature. Hence, the scatter of Hβ observed in cluster and luminous field elliptical galaxies can be explained by a spread in the metallicity of *old* stellar populations. We check our model with respect to the so-called G-dwarf problem in ellipticals. For a galaxy subsample covering a large range in $1500-V$ colors, we demonstrate that the addition of an old metal-poor subcomponent does not invalidate other observational constraints like colors and the flux in the mid-UV.

Subject headings: galaxies: abundances — galaxies: elliptical and lenticular, cD — galaxies: formation — galaxies: fundamental parameters — galaxies: stellar content

1. INTRODUCTION

More than 20 years ago it was recognized that the modeling of the spectral energy distribution of ellipticals is affected by an ambiguity in age and metallicity (Faber 1972; O'Connell 1976), which has turned out to be a general complication in population synthesis (Renzini 1986). However, considering Simple Stellar Populations (SSPs) in the two-parameter space of Balmer and metallic lines, the age-metallicity degeneracy can be broken (González 1993; Worthey 1994). The major reason for the success of this strategy is that the Balmer line strengths of SSPs are predominantly age sensitive at metallicities above $\sim\frac{1}{3}\ Z_{\odot}$, which are supposed to be the only metallicities relevant for elliptical galaxies. Strong Hβ lines are thus taken as an indication for young (intermediate-age) populations; the observed scatter is interpreted as a considerable spread in age (e.g., Faber et al. 1995).

An alternative path to obtaining blue stars and hence strong Balmer lines is to consider old *metal-poor* populations. In this paper we follow this approach and compute composite stellar populations that contain an old metal-poor subcomponent. The principal focus is to check if a combination of only old populations can reproduce strong Hβ without invalidating further constraints for ellipticals, like metallic indices, colors, and spectral energy distributions.

The paper is organized as follows. In § 2 we calibrate the SSP model indices and spectral energy distributions on globular cluster data. The composite models and their application to galaxy data are presented in § 3. In §§ 4 and 5 we discuss and summarize the results.

2. SIMPLE STELLAR POPULATION MODELS

We compute a new set of SSP models based on the population synthesis presented in Maraston (1998), in which the fuel consumption theorem (Renzini & Buzzoni 1986) is adopted to evaluate the energetics of the post–main-sequence phases. The new SSP models cover the metallicities $-2.25 < [\mathrm{Fe/H}] < 0.5$ and ages 10^7–2×10^{10} yr. The input stellar tracks are taken from Bono et al. (1997) and S. Cassisi (1999, private communication). These new models will be discussed in detail in a future paper (C. Maraston, in preparation). The calibration of the model colors on globular clusters is presented in Maraston (1998, 2000). Here we show the calibration of indices and spectral energy distributions of the SSP models that are relevant for the present study.

2.1. *Spectral Line Indices*

Synthetic line indices for SSPs are computed using the fitting functions from Worthey et al. (1994). Figure 1 shows Hβ, Fe5335, and Mg b as functions of [Fe/H] for galactic globular clusters from various data sets (see the legend of Fig. 1). Our SSP models of fixed-age (15 Gyr) and various metallicities are plotted as solid lines. Dotted lines are the models from Worthey (1994) for $t = 17$ Gyr.

As metal-poor stars ($[\mathrm{Fe/H}] \lesssim -1.3$) spend their horizontal-branch lifetimes at temperatures $T_{\mathrm{eff}} \gtrsim 5500$ K, Hβ is steeply rising with decreasing [Fe/H] (Fig. 1, *upper panel*). This observed feature is the key for the present analysis and is well reproduced by our SSPs. The models from Worthey (1994), instead, predict a shallower trend, which implies that the very metal-poor globulars are younger than the more metal-rich ones. The synthetic Fe5335 indices are in good agreement with the Covino, Galletti, & Pasinetti (1995) data, while for $[\mathrm{Fe/H}] \gtrsim -1.5$, Burstein et al. (1984) and Trager (1998) derive lower values. Mg b indices seem slightly overestimated by the models at low metallicities.

Our synthetic metallic indices Fe5335, Mg b, and the Balmer line Hβ for $[\mathrm{Fe/H}] \gtrsim -1.5$ agree well with the models from Worthey (1994), because both sets of models are based on the same fitting functions (Worthey et al. 1994). The uncertainty introduced by the use of different fitting functions is discussed in Maraston, Greggio, &

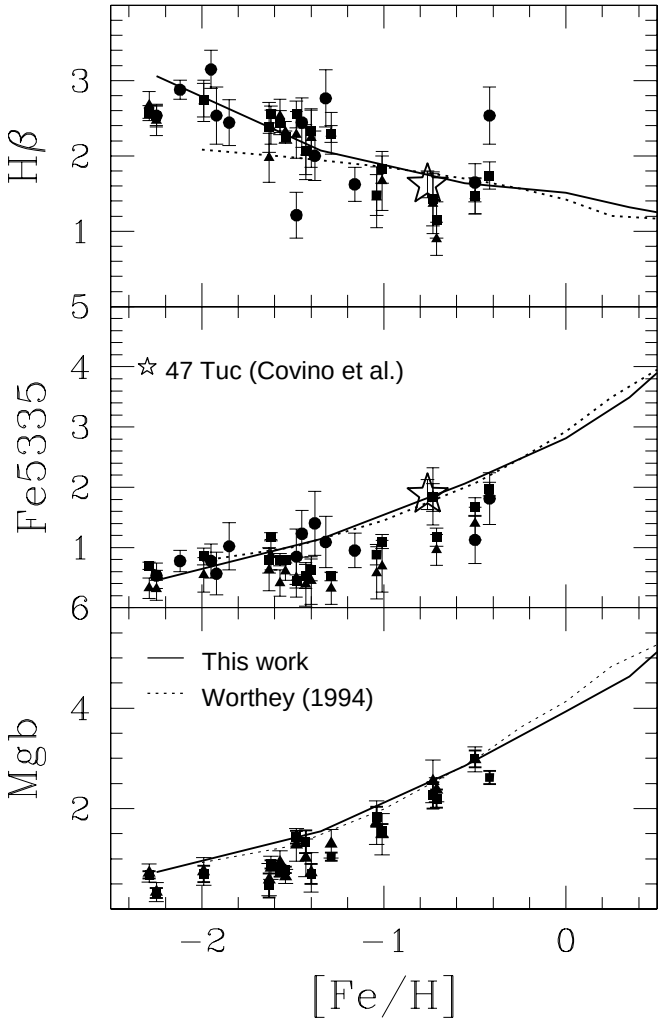

FIG. 1.—Calibration of the SSP models on galactic globular clusters. Data are from Burstein et al. (1984; *squares*), Covino et al. (1995; *circles*), and Trager (1998; *triangles*). [Fe/H] (Zinn & West 1984 scale) is taken from Harris (1996). Solid lines are our SSPs for age $t = 15$ Gyr. Worthey (1994) SSPs for $t = 17$ Gyr are shown as dotted lines.

Thomas (1999) and L. Greggio & C. Maraston (in preparation). The low Hβ values given by Worthey (1994) at very low metallicities are likely due to the assumption of too red horizontal-branch morphologies in the models.

As discussed in Worthey et al. (1994), iron indices are favorable as metallicity indicators, because the analysis with Mg indices is severely affected by α-enhancement (Tripicco & Bell 1995): SSP models based on solar abundance ratios predict—for a given Fe index—Mg indices weaker than those measured in elliptical galaxies (Worthey, Faber, & González 1992; Greggio 1997). As at high metallicities, the fitting functions of Fe5270 are significantly more uncertain (Maraston et al. 1999); in the following analysis we focus on Hβ and Fe5335. We additionally consider the color $B-K$ as metallicity indicator, which turns out to be in good agreement with Fe5335, while Mg b systematically implies higher metallicities (see § 3).

Combining Hβ with Fe5335, for 47 Tuc we obtain a "spectroscopic age" of 15 Gyr (Fig. 1), in agreement with the age derived from the color-magnitude diagram (14 ± 1 Gyr; Richer et al. 1996). This example shows that the Hβ-Fe5335 plane is successful in breaking the age-metallicity degeneracy when applied to simple systems like globular clusters. Note that the high-resolution Balmer index H$\gamma_{\rm HR}$, instead, leads to a "spectroscopic age" in excess of 20 Gyr (Gibson et al. 1999).

2.2. *Spectral Energy Distributions*

The evolutionary synthesis code of Maraston (1998) is updated for the computation of the SSP spectral energy distributions (SEDs). The spectral library of Lejeune, Cuisinier, & Buser (1998) is adopted to describe the stellar spectra as functions of gravity, temperature, and metallicity.

The tightest constraint on the amount and the metallicity of metal-poor stars in elliptical galaxies comes from the flux in the mid-UV (2000–4000 Å). In Figure 2 we present the calibration of synthetic metal-poor SEDs on galactic globular cluster data in the wavelength range $\lambda = 1500$–3300 Å (van Albada, de Boer, & Dickens 1981). The model spectra are in excellent agreement with the data in the whole metallicity range. The increase of the flux shortward 3000 Å with decreasing metallicity is due to a hotter main-sequence turnoff and a bluer horizontal branch. Note, however, that there are globulars of intermediate metallicity ([Fe/H] ~ -1.5) that show horizontal branches bluer than what it is expected with the canonical mass loss on the Red Giant Branch (RGB; van Albada et al. 1981). This case is shown in the central panel of Figure 2 for the globulars M13 (NGC 6205, *filled squares*) and NGC 5272, which have the same metallicity [Fe/H] ~ -1.54 but different horizontal-branch morphologies. M13 contains extreme blue horizontal-branch stars ("blue tails") and exhibits an excess of flux shortward ~ 2000 Å (see § 3.2.1).

As such blue tails are preferentially found in denser and more concentrated globulars, it is likely that the particular dynamical conditions in such "second parameter" globular clusters lead to enhanced mass loss and extremely hot horizontal-branch stars (Fusi Pecci et al. 1993), which may not apply to the average stellar field population in galaxies. Since in early-type galaxies globular clusters contribute less than 0.6% to the total V-light (Ashman & Zepf 1998), we adopt the canonical mass loss $\eta = 0.33$ for [Fe/H] ~ -1.5 calibrated on "normal" globulars like NGC 5272 (Fusi Pecci & Renzini 1975).

3. RESULTS

In the following we compare old (>12 Gyr) composite stellar populations with data of elliptical galaxies. The models consist of two components: a major metal-rich population ($Z = Z_{\rm maj}$) and a metal-poor subpopulation ($Z = Z_{\rm sub}$). More complex models with a continuum of metallicities will be the subject of a future paper.

3.1. *Indices and Colors*

Figure 3 displays Hβ versus Fe5335 (*left panel*) and Hβ versus $B-K$ (*right panel*) for composite models in which the ages of the major population and of the metal-poor subcomponent are fixed to 14 Gyr and 15 Gyr, respectively. The contribution from the low-metallicity population is 10% by mass. The grid in Figure 3 shows models for various metallicities of the two components. Solid lines connect models with constant metallicity of the major component, $Z_{\rm maj} = 0.5, 1, 2, 3\ Z_\odot$ (*from left to right*). The metallicity of the subcomponent is $Z_{\rm sub} = 0.05$ (*large, open squares*) and $Z_{\rm sub} = 0.005\ Z_\odot$ (*large, open circles*). For comparison, simple stellar populations with metallicities

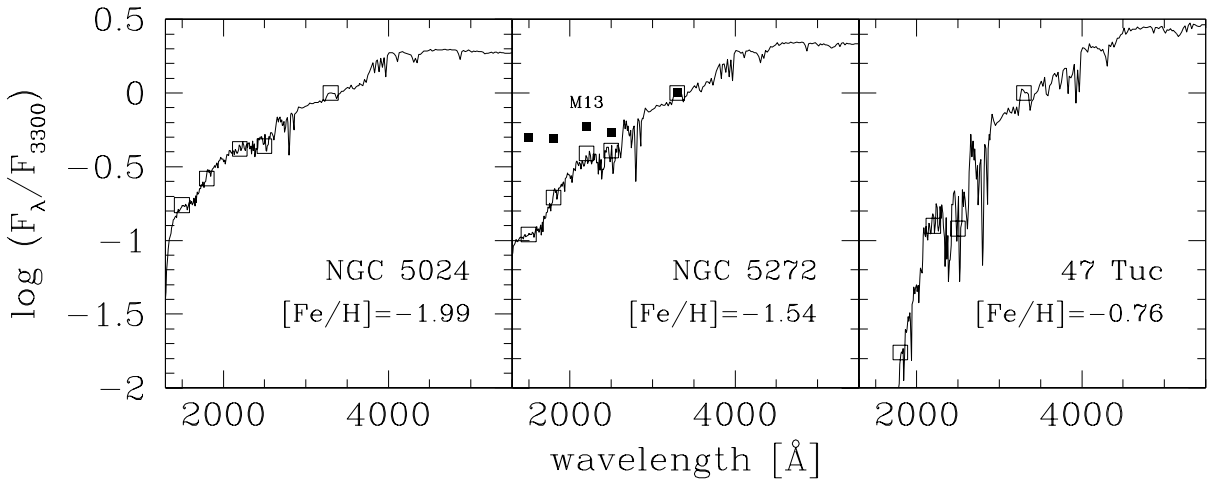

FIG. 2.—Calibration of the synthetic SEDs in the UV on galactic globular clusters. Data (*squares*) are taken from van Albada et al. (1981); [Fe/H] (Zinn & West 1984 scale) is adopted from Harris (1996). The filled squares (*central panel*) show M13 that has an extreme blue horizontal-branch morphology. The solid lines are our model SEDs ($t = 15$ Gyr) with metallicities as indicated in the panels.

$Z = Z_{\rm maj}$ and $t = t_{\rm maj}$ are shown as large, open triangles. The dotted (horizontal) lines mark models of constant $Z_{\rm sub}$.

The perturbation of metal-rich simple stellar populations with metal-poor stars leads to lower Fe5335 line strengths, bluer $B-K$ colors, and stronger Balmer lines. The models with $Z_{\rm sub} = 0.005\ Z_\odot$ reach H$\beta \sim 2$ Å. Observed line strengths (González 1993; Kuntschner & Davies 1998; Mehlert et al. 2000) and colors (Pahre 1998) of elliptical galaxies and lenticular galaxies are shown as small filled and small open symbols, respectively. The present set of composite models matches the area that is covered by the majority of the galaxy data. Note that the objects exhibiting H$\beta > 2$ Å either are classified as lenticular galaxies (*small, open symbols*) or are intermediate-mass *field* ellipticals (NGC 1700, NGC 3377, NGC 5831, NGC 6702, NGC 7454) or dwarf ellipticals (M32 [NGC 221], NGC 4489) from the González (1993) sample. All *luminous field ellipticals* and all *cluster ellipticals* (Coma, Fornax, and Virgo) in Figure 3, instead, can be modeled with the old composite populations introduced above. It should be emphasized that the bulk of ellipticals scatter around H$\beta \sim 1.6$ Å, so less than 10% contribution from metal-poor stars is required in most cases. The observed range H$\beta \sim 1.3$–2.0 is then due to a spread in the metallicity and/or the weight of the metal-poor subcomponent. The analysis with simple stellar population models, instead, yields an *age* spread of $\sim$7–15 Gyr.

Another striking feature of Figure 3 is that the positions of the galaxy data relative to each other are the same in the Fe5335 and the $B-K$ diagrams. Moreover, the locations of the model grids relative to the data points in the two panels are in good agreement, so that both the metallic index Fe5335 and the color $B-K$ consistently constrain the metallicity range for the major component to 1–3 $Z_\odot$. This strongly reinforces the use of Fe5335 as metallicity indicator (see § 2). In Figure 4 we show the same data and the same model grid in the Hβ-Mg b plane. As discussed in § 2.1, Mg lines of ellipticals are generally stronger than any SSP model. This feature is attributed to an enhancement of Mg in luminous ellipticals. As a consequence, the metallicities derived from the Mg-indices are substantially higher and provoke severe inconsistencies with observed colors (see also Saglia et al. 2000). As the latter are much less affected by abundance ratio anomalies, the Hβ–$B-K$ plane represents the more reliable constraint on stellar population models.

Note that the Hβ line index additionally suffers from uncertainties in the correction for contamination by emission (González 1993), which can lead to an underestimation of the Hβ line strength. This effect may explain the low values H$\beta \lesssim 1.5$ Å that fall below the model grid in Figure 3.

3.2. *Constraints from the Mid-UV*

The fluxes radiated by metal-poor stellar populations are high in the mid-UV (2000–4000 Å) and decrease shortward 2000 Å (Fig. 2). The so-called UV upturn below 2000 Å observed in elliptical galaxies (Burstein et al. 1988), instead, is most likely due to late evolutionary phases of old metal-rich populations (Greggio & Renzini 1990; Dorman, O'Connell, & Rood 1995; Yi, Demarque, & Oemler 1998; Greggio & Renzini 1999). The amount of metal-poor stars in elliptical galaxies is therefore tightly constrained by the flux in the mid-UV around 2500 Å.

A model based on the closed-box metallicity distribution is not compatible with the mid-UV flux of the elliptical galaxies NGC 4649 and NGC 1404 (Bressan, Chiosi, & Fagotto 1994) and of the M31 bulge (Worthey, Dorman, & Jones 1996), which is referred to as the G-dwarf problem for ellipticals. On the other hand, Lotz, Ferguson, & Bohlin (2000) find that the spectra of ellipticals in the mid-UV even require the addition of a metal-poor component. In the following we investigate if the proportions of metal-poor stars required to explain the Hβ line strengths are consistent with the fluxes observed in the mid-UV.

The objects with the strongest Hβ ($\sim$1.65) that we obtain from cross correlating the samples of González (1993), Kuntschner & Davies (1998), and Mehlert et al. (2000) with the Burstein et al. (1988) sample ("quiescent objects") are M31 (NGC 224), NGC 4472, and NGC 3379. We additionally consider NGC 4649, which exhibits a low H$\beta = 1.40$. These objects cover a large range in $1500-V$ colors, NGC 4649 having the strongest UV upturn. In the following we check if the composite models for these specific galaxies are in agreement with their SEDs. In order to con-

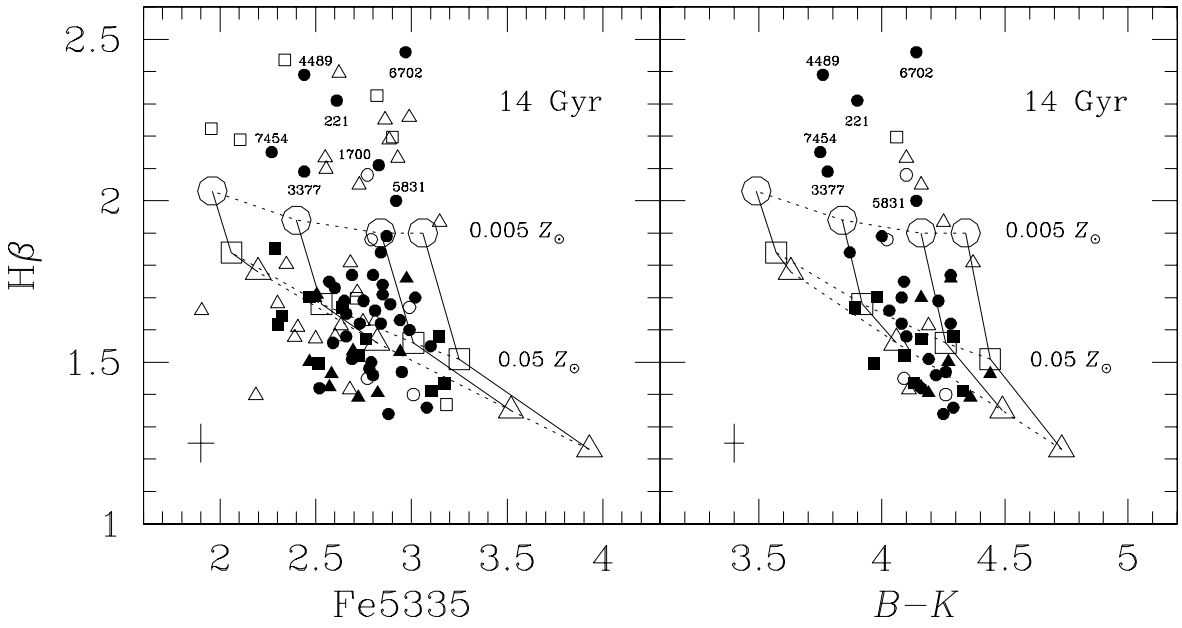

FIG. 3.—Hβ vs. Fe5335 and $B-K$ for elliptical (*small filled symbols*) and lenticular (*small open symbols*) galaxies. Data are from González (1993; *circles*, $R_e/8$ aperture, Virgo and field, labels indicate NGC numbers), Kuntschner & Davies (1998; *squares*, Fornax), and Mehlert et al. (2000; *triangles*, Coma). $B-K$ colors are taken from Pahre (1998). The error bars denote average 1σ errors. SSP models for $Z_{SSP} = 0.5, 1, 2, 3\ Z_\odot$ are large open triangles, with Z_{SSP} increasing from left to right. Composite models for $Z_{maj} = Z_{SSP}$ and $Z_{sub} = 0.05, 0.005\ Z_\odot$ are indicated by large open squares and large open circles. Solid and dotted lines denote fixed Z_{maj} and fixed Z_{sub}, respectively. The metal-poor subpopulation contributes 10% by mass. The ages of the major component and the subcomponent are 14 Gyr and 15 Gyr, respectively.

strain the flux from the metal-poor population in the mid-UV, it is necessary to model the UV upturn. Following the description by Greggio & Renzini (1990), we include hot ($T \sim 25{,}000$ K) late evolutionary phases in the metal-rich components, such that the observed UV rising branches are reproduced.

The main model parameters for each galaxy are listed in Table 1. Column (3) specifies the mass fractions (%) of the two components. Note that less than 10% is required in all cases. The metallicities, ages, indices (Hβ, Fe5335, Mg b), and colors ($B-K$, $U-V$) of the two populations are given in columns (4)–(10). The fuel F_{UV} (in $M_\odot$) in late evolutionary phases required in order to reproduce the observed UV upturn is given in column (11).

In Table 2 we present the relative contributions to Hβ and to the total fluxes at the wavelengths 5550 Å (V band), 3600 Å (U band), 2500 Å, and 1500 Å. The weight of the metal-poor component increases with decreasing λ, with a maximum contribution in the mid-UV ($\sim$2500 Å) as the rising branch shortward 2000 Å is produced by the metal-rich component. It is important to emphasize that in the model proposed here, the Balmer line strengths and the UV upturn do not have a common origin: we obtain strong Hβ with *metal-poor* (hot) horizontal-branch stars, while blue $1500-V$ colors are due to extremely hot, old *metal-rich* stars. The trend of decreasing Hβ with increasing Mg_2 and decreasing $1500-V$ (Burstein et al. 1988) is therefore not affected.

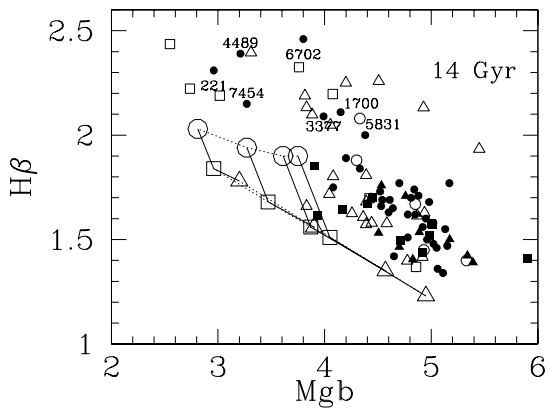

FIG. 4.—Hβ vs. Mg b. Symbols and line styles are like those in Fig. 3.

In Table 3 we compare the resulting indices and colors of the composed models with the observed values. The indices Hβ and Fe5335 and the colors $B-K$ and $U-V$ are in good agreement with observations.

The fits to the observed SEDs are shown in Figure 5 as thick solid lines; the dotted lines are the SEDs of the metal-poor and the metal-rich components. The spectra in the UV (*open symbols*) are from Burstein et al. (1988) and L. Buson (1999, private communication); the spectrophotometry in the optical (*thin solid lines*) is from D. Hamilton (1999, private communication). In all cases, the observed spectra are well reproduced in the full wavelength range $\lambda = 1200$–6000 Å. Thus the amount of metal-poor stars required in order to reproduce the observed Hβ (see Table 1) is consistent with the fluxes in the mid-UV; the model spectra perfectly match the minimum around 2500 Å. In the following we briefly discuss the individual galaxies.

3.2.1. *M31*

As shown in Table 1 we reproduce the observables of M31 (for the colors, see NGC 4472) with $Z_{sub} = 0.005\ Z_\odot$ contributing 3% to the total mass of the population, which

TABLE 1

MODEL PARAMETERS

Galaxy	Component	Mass (%)	Z ($Z_\odot$)	t (Gyr)	Hβ	Fe5335	Mg b	$B-K$	$U-V$	F_{UV} ($M_\odot$)
M31.....	Major	97	1.750	12	1.51	3.20	4.38	4.34	1.73	0.003
	Sub	3	0.005	15	3.09	0.53	0.78	2.64	0.53	...
N4472.....	Major	94	2.000	12	1.48	3.32	4.54	4.42	1.81	0.003
	Sub	6	0.030	15	2.33	1.02	1.38	2.91	0.72	...
N3379.....	Major	99	1.000	14	1.56	2.82	3.90	4.06	1.59	0.002
	Sub	1	0.005	15	3.09	0.53	0.78	2.64	0.53	...
N4649.....	Major	90	1.550	15	1.38	3.21	4.41	4.36	1.73	0.020
	Sub	10	0.300	15	1.69	2.08	2.87	3.53	1.15	...

TABLE 2

FLUX CONTRIBUTIONS

Galaxy	Hβ	5550 Å	3600 Å	2500 Å	1500 Å
M31.....	9	6	17	61	28
N4472.....	16	12	30	70	16
N3379.....	4	2	5	33	14
N4649.....	19	17	27	16	0

NOTE.—The table gives the relative contributions from the subcomponent (in %) to Hβ (col. [2]) and to the flux at the wavelengths specified in columns (3)–(6).

corresponds to 6% in V, 9% at Hβ, and 61% at $\lambda = 2500$ Å. Wu et al. (1980), instead, claim that not more than 50% contribution from a metal-poor component at $\lambda = 2500$ Å is compatible with the mid-UV flux of M31. The reason for this ostensible discrepancy is that the authors fix the metallicity of the metal-rich component to $Z_{maj} = 0.5\ Z_\odot$, which is lower than the value adopted here by more than a factor of 3 (see Table 1). As the SED of a more metal-rich population has lower flux in the mid-UV, our composite model requires a larger contribution from the metal-poor component. Using exactly the same prescriptions as these authors, we are consistent with their result. Because of the low metallicity of the metal-rich component, however, the model of Wu et al. (1980) fails in reproducing the other observational constraints of M31: it results in colors that are too blue ($B-K = 3.48$, $U-V \approx 1.21$), Fe indices that are too low (Fe5335 ≈ 2.01), and Balmer line strengths that are too high (H$\beta = 2.07$).

3.2.2. *NGC 4472*

The Virgo elliptical NGC 4472 has virtually the same properties as M31; therefore, it can be modeled with the same set of populations. The model given in the second line of Table 1 is an alternative option for both objects assuming a higher contribution from the metal-poor subcomponent and a higher metallicity of the major population. As a consequence, the contribution from the low-metallicity population increases to 70% at 2500 Å and to 12% in V. Wu et al. (1980) derive a lower contribution in V relative to 2500 Å (50% at 2500 Å and 6% in V), because the authors chose the globular cluster M13 (NGC 6205) as a representative of the metal-poor population. As discussed in § 2.2, this particular globular cluster has an extreme blue horizontal-branch morphology and exhibits very high fluxes in the mid-UV (see Fig. 2), which implies a lower V over 2500 Å flux ratio.

3.2.3. *NGC 3379*

NGC 3379 exhibits equally high Hβ but bluer colors and lower metallic indices. The best fitting model thus has a lower $Z_{maj} = Z_\odot$ and requires only 1% of $Z_{sub} = 0.005\ Z_\odot$.

3.2.4. *NGC 4649*

NGC 4649 has the strongest UV upturn (bluest $1500-V$), requiring a factor of ~ 10 more fuel at late evolutionary phases than the other cases do (see col. [11] in Table 1). Given the low Hβ line strength, the best fit is obtained with a model containing only old metal-rich populations ($Z_{sub} = 0.3\ Z_\odot$). This object strongly supports the view that the UV rising branch and Hβ line strength are not produced by the same kind of stars.

3.3. *Models for* H$\beta > 2$ Å

The model grid in Figure 3 extends to H$\beta \approx 2$ Å, while some low-mass field ellipticals exhibit stronger Balmer lines. In principle such high Hβ can be obtained by increasing the weight of the low-metallicity component. For instance, the compact dwarf elliptical M32 (NGC 221) with H$\beta = 2.37 \pm 0.12$ and Fe5335 $= 2.54 \pm 0.20$ (Kormendy & Bender 1999) can be modeled by the 14 Gyr old two-

TABLE 3

RESULTS

	Hβ		Fe5335		$B-K$		$U-V$	
GALAXY	Model	Observed	Model	Observed	Model	Observed	Model	Observed
M31.....	1.65	1.67 ± 0.07	3.04	2.99 ± 0.06	4.26	...	1.61	...
N4472.....	1.62	1.62 ± 0.06	3.04	2.84 ± 0.08	4.28	4.28	1.59	1.57
N3379.....	1.62	1.62 ± 0.05	2.77	2.73 ± 0.04	4.05	4.08	1.55	1.52
N4649.....	1.44	1.40 ± 0.05	3.01	3.01 ± 0.05	4.24	4.26	1.61	1.61

NOTE.—Indices and colors of the models given in Table 1. Index data (1 σ errors) are from González 1993, $B-K$ from Pahre 1998, and $U-V$ from Trager 1998.

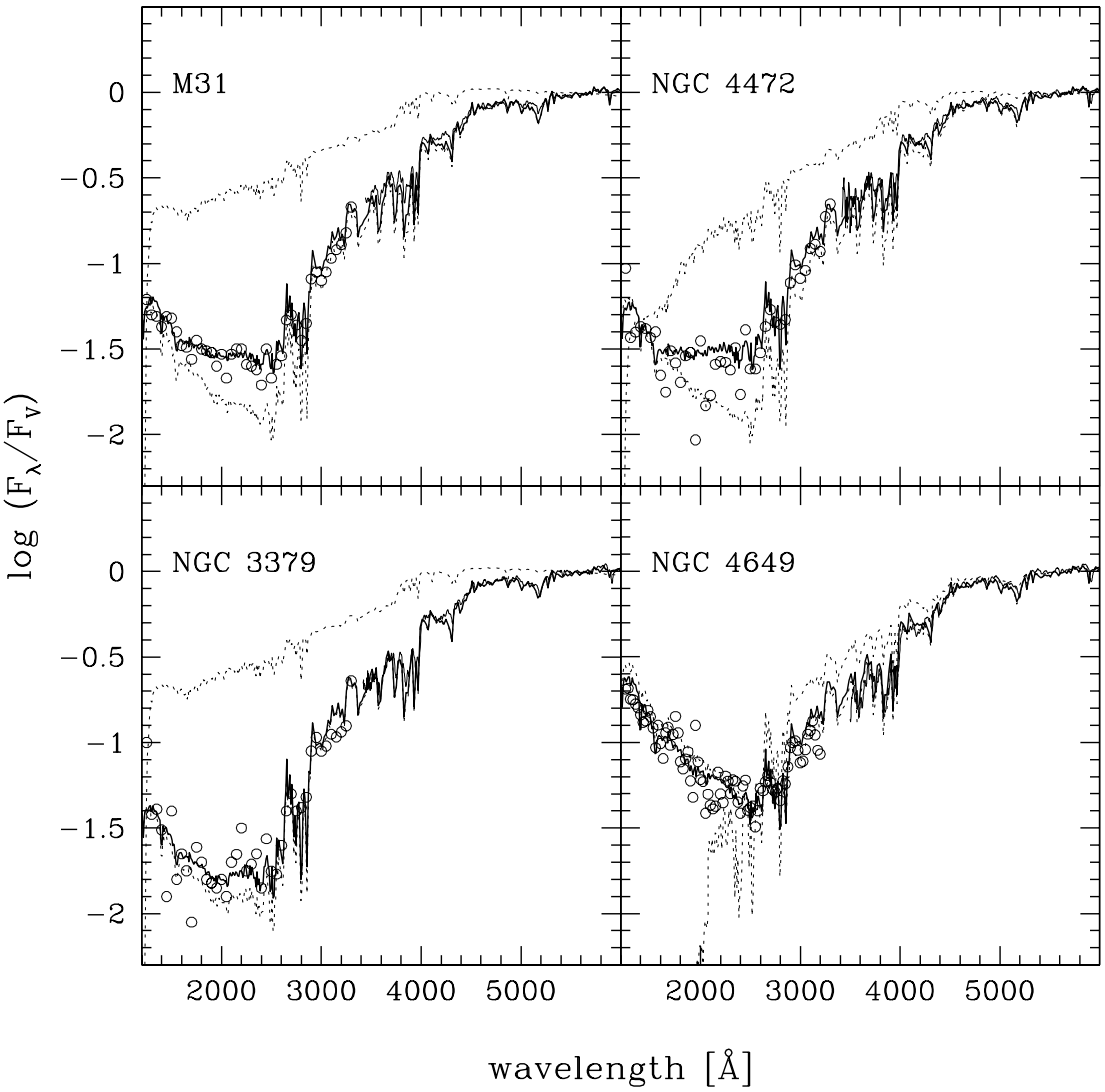

FIG. 5.—Spectral energy distributions as a function of wavelength. *IUE* data for $\lambda \leq 3300$ Å (*circles*) are from Burstein et al. (1988) and L. Buson (1999, private communication); the spectrophotometry for $\lambda \geq 3440$ Å (*thin solid lines*) is from D. Hamilton (1999, private communication). The models from Table 1 are shown as thick solid lines; dotted lines are the SEDs of the metal-poor and the metal-rich components (100%), respectively.

component population with $Z_{\rm maj} = 2$–$3\ Z_\odot$ and 20% of $Z_{\rm sub} = 0.005\ Z_\odot$. The SED of this model with such a large fraction of very metal-poor stars, however, is not compatible with the fluxes observed in the mid-UV (see also Burstein et al. 1984; Rose & Deng 1999). On the other hand, from a deep *Hubble Space Telescope* (*HST*) color-magnitude diagram, Grillmair et al. (1996) conclude that there is no evidence for an intermediate-age population ($t \lesssim 2$ Gyr). It is worth mentioning, however, that M32 is a peculiar object that does not have the properties of the average elliptical galaxy population.

Alternatively to the addition of metal-poor stars, metal-rich populations with blue horizontal-branch morphologies could reproduce strong Hβ without invoking young ages. Such hot horizontal-branch stars are indeed observed in the metal-rich globular clusters NGC 6388 and NGC 6441 of the galactic bulge (Rich et al. 1997) and in M32 (Brown et al. 2000). A possible mechanism to produce these temperatures is enhanced mass loss along the RGB evolutionary phase. The investigation of this channel to obtain strong Hβ in old metal-rich populations will be the subject of a future paper.

4. DISCUSSION

4.1. *Metallicity Distributions in Ellipticals*

The principle idea of this paper is to enhance the Balmer line strengths of old metal-rich stellar populations with a small fraction of metal-poor stars. The real metallicity distribution of the stellar populations in elliptical galaxies is difficult to assess observationally, as the stars cannot be resolved. The *HST* color-magnitude diagram of M32 (Grillmair et al. 1996) and the spectroscopy of K giants in the bulge (Rich 1988) show that these spheroids contain a tail of low-metallicity stars. The closest giant elliptical for which color-magnitude diagrams are available is NGC 5128 (Harris, Harris, & Poole 1999). Analyzing deep *HST* images in the outer halo of NGC 5128, the authors find a differential metallicity distribution that is well reproduced by two closed box–like chemical enrichment scenarios implying a large number of extremely metal-poor stars. In particular the differential shape of the distribution implies a formation picture in which a metal-poor and a metal-rich population are formed separately from each other.

This picture gets further support from a number of studies that discover bimodal color and metallicity distributions of globular clusters in at least half of the early-type galaxy population (Zepf & Ashman 1993; Gebhardt & Kissler-Patig 1999). Spectroscopic and photometric investigations indicate that both populations are old (Kissler-Patig et al. 1998b; Cohen, Blakeslee, & Ryzhov 1998; Kissler-Patig, Forbes, & Minniti 1998a; Kundu et al. 1999; Puzia et al. 1999). More specifically, Puzia et al. (1999) find that the two populations in NGC 4472 are old and coeval, with metallicities $\sim 0.05\, Z_\odot$ and $\sim Z_\odot$. In the framework of hierarchical structure formation, galaxies are built by mergers of smaller objects (e.g., White & Rees 1978; White & Frenk 1991; Kauffmann, White, & Guiderdoni 1993). A merger of coeval systems without newly induced star formation would result in a coeval composite population. The accretion of a dwarf galaxy by a larger system (minor merger) qualitatively explains the existence of a metal-poor subpopulation.

There is an additional important effect that is independent of the assumed scheme of galaxy formation. As discussed by Greggio (1997), a sizable fraction of metal-poor stars from the outer parts of a galaxy contaminate the light coming from the center because of projection and orbital mixing (Ciotti, Stiavelli, & Braccesi 1995). The authors find that projection effects lower the actual central metallicity by roughly 10%. The metal-poor components in the composite models of M31, NGC 4472, and NGC 3379 (Table 1) dilute the metallicities of the metal-rich populations by 3%, 6%, and 4%, respectively. Projection effects alone thus may be sufficient to explain the amount of metal-poor stars considered in the present analysis.

4.2. *Evidence against Recent Star Formation*

There are observational indications from the fundamental plane (Djorgovski & Davis 1987; Dressler et al. 1987; Bender, Burstein, & Faber 1992, 1993; Renzini & Ciotti 1993) and the color-magnitude relation (Bower, Lucey, & Ellis 1992) that limit the fraction of the young population to less than 10%. As late star formation leads to low α/Fe ratios (Thomas, Greggio, & Bender 1999; Thomas 1999), the addition of a young population provokes inconsistencies with the high α/Fe ratios observed in elliptical galaxies (e.g., Worthey et al. 1992). Also, the redshift evolution of colors (Aragón Salamanca et al. 1993) of the Mg-σ relation (Bender, Ziegler, & Bruzual 1996) of the Kormendy relation (Ziegler et al. 1999) and of the color gradients in cluster ellipticals (Saglia et al. 2000) leave little space for a significant contribution from a young subcomponent. The addition of an old, metal-poor population as discussed in this paper can reconcile these findings with strong Balmer lines.

Disturbed field ellipticals that have strong Hβ absorption (Schweizer et al. 1990) and blue optical colors (Schweizer & Seitzer 1992) do not show any signature of recent star formation activity in the infrared colors (Silva & Bothun 1998a, 1998b). As discussed by these authors, recent mergers may not have been accompanied by significant star formation, but metallicity effects are favored to explain the enhanced Hβ line strengths.

5. SUMMARY

In this paper we show that strong Balmer lines can be produced by composite populations that contain a small fraction of old *metal-poor* stars.

The key to this result is that at low metallicities and old ages our SSP models show a steep increase of Hβ with decreasing metallicity, in accordance with what is observed in metal-poor globular clusters. We compute composite stellar population models that consist of an underlying old metal-rich population and a small fraction of an old metal-poor subcomponent. Assuming a 10% contribution from metal-poor stars, we construct a grid of models in the Hβ-Fe5335 and the Hβ–$B-K$ planes that reproduces Hβ up to 2 Å and covers most of the elliptical galaxy data. It should be emphasized that the same conclusion holds for all Balmer lines, e.g., Hγ and Hδ. More specifically, the data of all cluster and luminous field ellipticals can be explained by our models without invoking young ages. The scatter in Balmer line strengths is then caused by a spread in the metallicity and/or the weight of the metal-poor component. Most ellipticals can be modeled with less than 10% of metal-poor stars as the data scatter about H$\beta \sim 1.6$ Å.

We further show that the spectral energy distributions of the composite models that reproduce the indices and colors of representative examples agree well with the observed spectra in the wavelength range 1200–6000 Å. Our models are perfectly compatible with the observed minimum at 2500 Å that tightly constrains the possible amount of metal-poor stars.

We conclude that the age-metallicity degeneracy for complex systems like elliptical galaxies still remains to be solved. The perturbation with old *metal-poor* stars to obtain strong Balmer lines is alternative to the addition of a *young* metal-rich population (e.g., de Jong & Davies 1997; Kuntschner 2000; Longhetti et al. 2000). The key to discriminate between the two options lies in the evolution of Balmer lines with redshift. A young population of 2–5 Gyr should leave its fingerprints with a significant peak of Balmer line strengths at redshifts $z \sim 0.15$–0.4, depending on the cosmology, which has not been detected so far (Ziegler & Bender 1997). The model presented here, instead, predicts Balmer lines to become monotonically stronger with redshift.

We are grateful to S. Cassisi, D. Hamilton, D. Mehlert, and L. Buson for providing electronic versions of models and data. We thank R. Bender and M. Kissler-Patig for the careful reading of the manuscript. For many helpful discussions, we thank N. Drory, L. Greggio, U. Hopp, and R. Saglia. The referee is acknowledged for the very useful comments that improved the first version of the paper. This work was supported by the "Sonderforschungsbereich 375-95 für Astro-Teilchenphysik" of the Deutsche Forschungsgemeinschaft.

REFERENCES

Aragón Salamanca, A., Ellis, R. S., Couch, W. J., & Carter, D. 1993, MNRAS, 262, 764
Ashman, K. M., & Zepf, S. E. 1998, Globular Cluster Systems (Cambridge: Cambridge Univ. Press)
Bender, R., Burstein, D., & Faber, S. M. 1992, ApJ, 399, 462
———. 1993, ApJ, 411, 153
Bender, R., Ziegler, B. L., & Bruzual, G. 1996, ApJ, 463, L51
Bono, G., Caputo, F., Cassisi, S., Castellani, V., & Marconi, M. 1997, ApJ, 489, 822
Bower, R. G., Lucey, J. R., & Ellis, R. S. 1992, MNRAS, 254, 589
Bressan, A., Chiosi, C., & Fagotto, F. 1994, ApJS, 94, 63
Brown, T. M., Bowers, C. W., Kimble, R. A., Sweigart, A. V., & Ferguson, H. C. 2000, ApJ, 532, 308
Burstein, D., Bertola, F., Buson, L. M., Faber, S. M., & Lauer, T. R. 1988, ApJ, 328, 440
Burstein, D., Faber, S. M., Gaskell, C. M., & Krumm, N. 1984, ApJ, 287, 586
Ciotti, L., Stiavelli, M., & Braccesi, A. 1995, MNRAS, 276, 961
Cohen, J. G., Blakeslee, J. P., & Ryzhov, A. 1998, ApJ, 496, 808
Covino, S., Galletti, S., & Pasinetti, L. E. 1995, A&A, 303, 79
de Jong, R. S., & Davies, R. L. 1997, MNRAS, 285, L1
Djorgovski, S., & Davis, M. 1987, ApJ, 313, 59
Dorman, B., O'Connell, R. W., & Rood, R. T. 1995, ApJ, 442, 105
Dressler, A., Lynden-Bell, D., Burstein, D., Davies, R. L., Faber, S. M., Terlevich, R. J., & Wegner, G. 1987, ApJ, 313, 42
Faber, S. M. 1972, A&A, 20, 361
Faber, S. M., Trager, S. C., González, J. J., & Worthey, G. 1995, in IAU Symp. 164, Stellar Populations, ed. P. C. Van der Kruit & G. Gilmore (Dordrecht: Kluwer), 249
Fusi Pecci, F., Ferraro, F. R., Bellazzini, M., Djorgovski, S., Piotto, G., & Buonanno, R. 1993, AJ, 105, 1145
Fusi Pecci, F., & Renzini, A. 1975, A&A, 39, 413
Gebhardt, K., & Kissler-Patig, M. 1999, AJ, 118, 1526
Gibson, B. K., Madgwick, D. S., Jones, L. A., Da Costa, G. S., & Norris, J. E. 1999, AJ, 118, 1268
González, J. 1993, Ph.D. thesis, Univ. California, Santa Cruz
Greggio, L. 1997, MNRAS, 285, 151
Greggio, L., & Renzini, A. 1990, ApJ, 364, 35
———. 1999, Mem. Soc. Astron. Italiana, 70, 691
Grillmair, C. J., et al. 1996, AJ, 112, 1975
Harris, G. L. H., Harris, W. E., & Poole, G. B. 1999, AJ, 117, 855
Harris, W. E. 1996, AJ, 112, 1487
Kauffmann, G., White, S. D. M., & Guiderdoni, B. 1993, MNRAS, 264, 201
Kissler-Patig, M., Forbes, D. A., & Minniti, D. 1998a, MNRAS, 298, 1123
Kissler-Patig, M., et al. 1998b, AJ, 115, 105
Kormendy, J., & Bender, R. 1999, ApJ, 522, 772
Kundu, A., Whitmore, B. C., Sparks, W. B., Macchetto, F. D., Zepf, S. E., & Ashman, K. M. 1999, ApJ, 513, 733
Kuntschner, H. 2000, MNRAS, 315, 184
Kuntschner, H., & Davies, R. L. 1998, MNRAS, 295, L29
Lejeune, T., Cuisinier, F., & Buser, R. 1998, A&AS, 130, 65
Longhetti, M., Bressan, A., Chiosi, C., & Rampazzo, R. 2000, A&A, 353, 917
Lotz, J. M., Ferguson, H. C., & Bohlin, R. C. 2000, ApJ, 532, 830
Maraston, C. 1998, MNRAS, 300, 872
———. 2000, in The Chemical Evolution of the Milky Way: Stars versus Clusters, ed. F. Giovannelli & F. Matteucci (Dordrecht: Kluwer)
Maraston, C., Greggio, L., & Thomas, D. 2000, Ap&SS, in press (astro/ph-9906088)
Mehlert, D., Saglia, R. P., Bender, R., & Wegner, G. 2000, A&AS, 141, 449
O'Connell, R. W. 1976, ApJ, 206, 370
Pahre, M. A. 1998, Ph.D. thesis, California Institute of Technology
Puzia, T. H., Kissler-Patig, M., Brodie, J. P., & Huchra, J. P. 1999, AJ, 118, 2734
Renzini, A. 1986, in Stellar Populations, ed. C. A. Norman, A. Renzini, & M. Tosi (Cambridge: Cambridge Univ. Press), 213
Renzini, A., & Buzzoni, A. 1986, in Spectral Evolution of Galaxies, ed. C. Chiosi & A. Renzini (Dordrecht: Reidel), 135
Renzini, A., & Ciotti, L. 1993, ApJ, 416, L49
Rich, R. M. 1988, AJ, 95, 828
Rich, R. M., et al. 1997, ApJ, 484, L25
Richer, H. B., et al. 1996, ApJ, 463, 602
Rose, J. A., & Deng, S. 1999, AJ, 117, 2213
Saglia, R. P., Maraston, C., Greggio, L., Bender, R., & Ziegler, B. 2000, A&A, in press (astro-ph 0007038)
Schweizer, F., & Seitzer, P. 1992, AJ, 104, 1039
Schweizer, F., Seitzer, P., Faber, S. M., Burstein, D., Dalle Ore, C. M., & González, J. J. 1990, ApJ, 364, L33
Silva, D. R., & Bothun, G. D. 1998a, AJ, 116, 85
———. 1998b, AJ, 116, 2793
Thomas, D. 1999, MNRAS, 306, 655
Thomas, D., Greggio, L., & Bender, R. 1999, MNRAS, 302, 537
Trager, S. C. 1998, Ph.D. thesis, Univ. California, Santa Cruz
Tripicco, M. J., & Bell, R. A. 1995, AJ, 110, 3035
van Albada, T. S., de Boer, K. S., & Dickens, R. J. 1981, MNRAS, 195, 591
White, S. D. M., & Frenk, C. S. 1991, ApJ, 379, 52
White, S. D. M., & Rees, M. J. 1978, MNRAS, 183, 341
Worthey, G. 1994, ApJS, 95, 107
Worthey, G., Dorman, B., & Jones, L. A. 1996, AJ, 112, 948
Worthey, G., Faber, S. M., & González, J. J. 1992, ApJ, 398, 69
Worthey, G., Faber, S. M., González, J. J., & Burstein, D. 1994, ApJS, 94, 687
Wu, C. C., Faber, S. M., Gallagher, J. S., Peck, M., & Tinsley, B. M. 1980, ApJ, 237, 290
Yi, S., Demarque, P., & Oemler, A., Jr. 1998, ApJ, 492, 480
Zepf, S. E., & Ashman, K. E. 1993, MNRAS, 264, 611
Ziegler, B. L., & Bender, R. 1997, MNRAS, 291, 527
Ziegler, B. L., Saglia, R. P., Bender, R., Belloni, P., Greggio, L., & Seitz, S. 1999, A&A, 346, 13
Zinn, R., & West, M. J. 1984, ApJS, 55, 45